

Topology, chiral and screening transitions at finite density in two colour QCD

B. Allés^{a*}, M. D’Elia^b and M. P. Lombardo^c

^aINFN, Sezione di Pisa, Pisa, Italy

^bDipartimento di Fisica, Università di Genova and INFN, Genova, Italy

^cINFN, Laboratori Nazionali di Frascati, Frascati, Italy

The behaviour of the topological susceptibility in QCD with two colours and 8 flavours of quarks is studied at nonzero temperature on the lattice across the finite density transition. It is shown that its signal drops at a (pseudo-)critical chemical potential μ_c . The Polyakov loop and the chiral condensate undergo their transitions at the same value. Pauli blocking supervenes at a value of the chemical potential larger than μ_c .

1. INTRODUCTION

The phase space of QCD in the temperature and quark chemical potential μ plane is shown schematically in Fig. 1. Many of the transition lines and phases displayed in the Figure are theoretical predictions with little experimental verification. We have studied the transition as the chemical potential is varied (dashed arrow in Fig. 1) at a fixed temperature T that is most likely above the region where a diquark condenses.

We wanted to understand the fate of the topological susceptibility χ across the transition and to decide whether its possible change occurs at the same value of μ where the vector chiral symmetry is restored and the Polyakov loop signal rises [1].

It is known that at the finite temperature transition the signal of χ drops abruptly for Yang–Mills theory [2,3] as well as for QCD with several values of the flavour number N_f [4]. The present is the first work where a similar study is performed at the finite density transition (the full account can be found in Ref. [5]).

We have performed the study on the lattice by simulating the theory with two colours in order to avoid the sign problem that in the three colour theory makes the importance sampling method impracticable (for methods to overcome

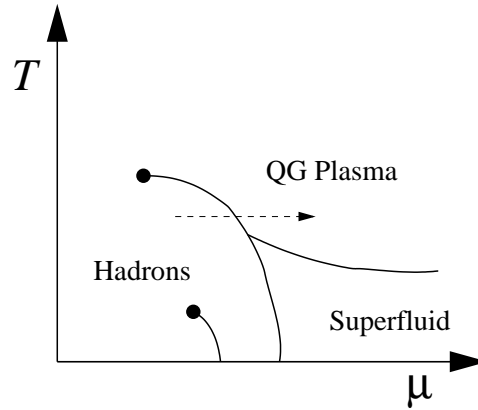


Figure 1. Sketch of the T - μ phase diagram in QCD with two colours. We have studied the transition crossed by the dashed arrow at finite temperature as the density is varied.

this problem see [6] and references therein). We expect that this modification of true QCD has little impact on the results concerning gluon properties and in particular instanton physics. The main differences between two and three colour QCD regard aspects of the theory that we have not studied, like the hadron spectrum and the diquark condensed phase [7,8]. In fact in the two colour theory mesons are degenerate with baryons (which are made of two quarks) and the

*Speaker at the conference.

diquark condensate phase becomes superfluid instead of superconducting because two quarks in two colour QCD can create a colour blind condensate.

2. SIMULATION AND OBSERVABLES

We have simulated the model on a $14^3 \times 6$ lattice at an inverse bare lattice gauge coupling $\beta = 4/g^2 = 1.5$ and quark mass $am = 0.07$ in units of lattice spacing a . The Wilson action was used for gauge fields and the standard action for 8 flavours of quarks in the staggered formulation.

The Hybrid Molecular Dynamics algorithm was chosen to update configurations. They were separated typically by 50–100 steps of the algorithm in order to well decorrelate the topology [9,10,11]. We followed the behaviour of several observables across the transition shown in Fig. 1: chiral condensate $\langle \bar{\psi}\psi \rangle$, Polyakov loop or Wilson line P , topological susceptibility χ , baryonic density ρ_B and average plaquette $\text{Tr } \square/2$

2.1. Topology

The measurement of the topological susceptibility requires a careful treatment of composite operators. This quantity is defined as

$$\chi \equiv \int d^4x \langle T \{ Q(x) Q(0) \} \rangle, \quad (1)$$

where $Q(x)$ is the topological charge density operator that appears in the r.h.s. of the axial singlet anomaly. χ is related to the η' mass through the Witten–Veneziano mechanism [12,13] and to the chiral condensate in the massless limit [14].

Eq.(1) can be rewritten in a more compact form,

$$\chi = \frac{\langle Q^2 \rangle}{V}, \quad (2)$$

where the total topological charge Q is defined as $Q \equiv \int d^4x Q(x)$ and V is the spacetime volume. This expression has only a formal meaning because it must be supplemented with a multiplicative renormalization for each power of the topological charge operator Q [15,16] as well as a careful treatment of the contact divergences that appear when the two operators are evaluated at the same spacetime point [17].

A detailed description of the procedure that we have followed to extract χ can be found in [5]. In a nutshell, one has to define a lattice regularization $Q_L(x)$ of the topological charge density operator. The corresponding total lattice topological charge is $Q_L = \sum_x Q_L(x)$ and the lattice topological susceptibility is $\chi_L = \langle Q_L^2 \rangle / V$. This quantity is related to the physical susceptibility χ by the general expression [15,16,17]

$$\chi_L = Z^2 a^4 \chi + M, \quad (3)$$

where Z is a multiplicative renormalization of Q_L , a is the lattice spacing and M is an additive renormalization constant. In presence of composite operators the usual renormalization program in a renormalizable theory is not enough to fully renormalize a Green's function. This is the origin of Z (even in the case of the pure gauge theory where the topological charge operator has no anomalous dimensions). On the other hand part of the contact divergences that appear in the product of the two topological charge operators must be subtracted. This subtraction is defined as $M \equiv \chi_L|_{Q=0}$, i.e. M is the value of χ_L in the sector of zero topological charge. This condition guarantees the obvious requirement that χ vanishes in that sector.

2.2. Calculation of Z and M

One has to calculate the two constants Z and M and insert them into Eq.(3) in order to extract χ . We shall present the results in the form of the ratio $\chi(\mu)/\chi(\mu=0)$ as a function of μ . Therefore we need not calculate Z and only M is required. This additive renormalization constant was computed by using a non-perturbative method [18,19,3]. It is enough to calculate it for one single value of the chemical potential because M is independent of infrared properties.

3. RESULTS

In Fig. 2 we show the resulting behaviour of the topological susceptibility as a function of the chemical potential. A clear cut drop is seen at the position $a\mu_c = 0.175(5)$. This sudden fall is an indication of the effective restoration of the axial singlet symmetry [20].

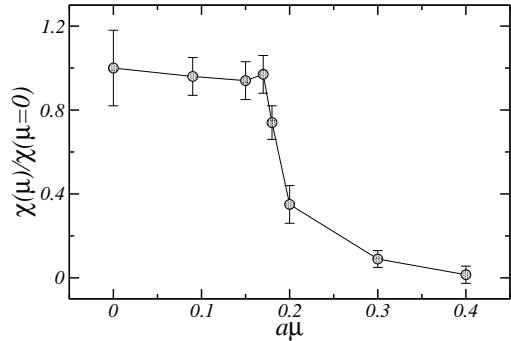


Figure 2. The ratio $\chi(\mu)/\chi(\mu=0)$ as a function of $a\mu$ showing the abrupt drop of the signal of the topological susceptibility at a (pseudo-) critical value of the chemical potential.

We do not show the analogous figures for the Polyakov loop and chiral condensate behaviours (see Ref. [5]). Instead in Fig. 3 the derivatives of the three quantities (topological susceptibility, Polyakov loop and chiral condensate) are superimposed to give evidence of the coincidence of the three transitions: they all happen at the same (pseudo-)critical value $a\mu_c = 0.175(5)$. Single points are the result of the discrete derivatives computed from the measured data while the lines are the derivatives of the interpolations made with a natural cubic spline on each data set. Since the theory deconfines at the same μ where $\langle\bar{\psi}\psi\rangle$ vanishes, the path in the T - μ diagram followed in our study possibly lies above the superfluid phase (as indicated in Fig. 1) [21].

3.1. Numerical results

In order to give an estimate of the main results in physical units, we have done a second simulation of the model at zero chemical potential by varying the inverse bare lattice coupling β on the same lattice volume and have measured the Polyakov loop and chiral condensate. The data clearly reflected the existence of a critical $\beta_c = 1.594(6)$. It was then assumed that the corresponding transition temperature T_c lies in the range 100–200 MeV. Hence a value for the lattice spacing at β_c was obtained. This value

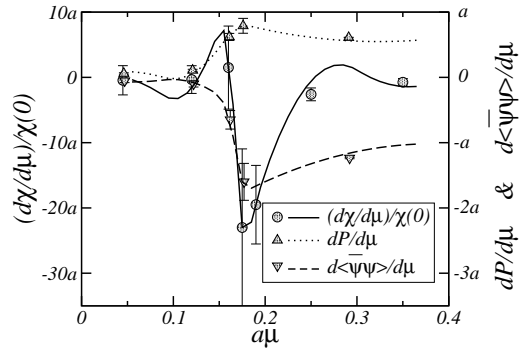


Figure 3. Derivatives with respect to the chemical potential μ of the normalized topological susceptibility (circles, continuous line and left vertical axis), Polyakov loop (up triangles, dotted line and right vertical axis) and chiral condensate (down triangles, dashed line and right vertical axis). The two vertical axes are expressed in units of the lattice spacing a . The three sets of data have been slightly shifted horizontally to avoid the overlapping of various symbols and error bars. Lines are the result of a spline interpolation.

was then run, by making use of the two-loop beta function, from β_c to our working $\beta = 1.5$ thus obtaining the lattice spacing at this beta $a(\beta = 1.5) = 0.64(4)({}_{-16}^{+33})$ fm (errors derived from the imprecision on β_c and from the inaccuracy of the estimate for T_c respectively).

This result allowed us to assign physical units to the various parameters of our simulation: $\mu_c = 54(2)(4)(18)$ MeV (errors are respectively due to the estimate of $a\mu_c$, the imprecision on β_c and the rough approximation of T_c) and $T = 51(4)(17)$ MeV (error on β_c and on T_c respectively).

Notice that the numerical value of μ_c is roughly compatible with half of the mass of the lightest baryon (in the two colour theory it is made of two quarks and degenerated with the pion). However we take the above numbers with caution because of the large systematic errors derived from the small and coarse lattice volume, the (wrong) gauge group and the inexact updating algorithm.

3.2. Pauli blocking

By repeating the simulation at very high values of the chemical potential, in principle one could test the perturbative region of the phase diagram. However the advent of the so-called Pauli blocking makes that not viable. As μ increases, more and more fermions are placed in the lattice volume. Since it contains a countable number of sites, the Pauli principle imposes a maximum allowed number of fermions that can be placed on them. In our case the maximum allowed density is one baryon per site [22]. This maximum is attained for $a\mu_s \approx 1.2$. After that point, fermions are frozen and the theory becomes entirely quenched. We have verified this statement by calculating the baryon density and the average plaquette. Their data are shown in Fig. 4. ρ_B becomes 1 and stays constant for all $\mu > \mu_s$. Also the average plaquette stays constant after μ_s and this constant coincides with the value obtained from a separate Monte Carlo study where the pure gauge theory was simulated (represented by the down triangle in Fig. 4). We stress that Pauli blocking is a lattice effect with no counterpart in the continuum.

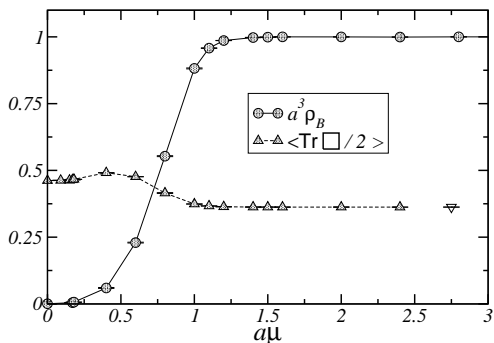


Figure 4. Baryon density per space site and average plaquette as a function of $a\mu$. The down triangle is the result of a separate simulation for the pure gauge theory.

REFERENCES

1. E. Shuryak, Comments Nucl. Part. Phys. 21 (1994) 235.
2. B. Allés, M. D’Elia, A. Di Giacomo, Phys. Lett. B412 (1997) 119.
3. B. Allés, M. D’Elia, A. Di Giacomo, Nucl. Phys. B494 (1997) 281, Erratum: ibid B679 (2004) 397.
4. B. Allés, M. D’Elia, A. Di Giacomo, Phys. Lett. B483 (2000) 139.
5. B. Allés, M. D’Elia, M. P. Lombardo, Nucl. Phys. B752 (2006) 124.
6. E. Laermann, O. Philipsen, Ann. Rev. Nucl. Part. Sci. 53 (2003) 163.
7. S. Hands, J. B. Kogut, M. P. Lombardo, S. E. Morrison, Nucl. Phys. B558 (1999) 327.
8. J. B. Kogut, M. A. Stephanov, D. Toublan, J. J. M. Verbaarschot, A. Zhitnitsky, Nucl. Phys. B582 (2000) 477.
9. B. Allés, G. Boyd, M. D’Elia, A. Di Giacomo, E. Vicari, Phys. Lett. B389 (1996) 107.
10. B. Allés et al., Phys. Rev. D58 (1998) 071503.
11. Y. Aoki et al., Phys. Rev. D72 (2005) 114505.
12. E. Witten, Nucl. Phys. B156 (1979) 269.
13. G. Veneziano, Nucl. Phys. B159 (1979) 213.
14. F. C. Hansen, H. Leutwyler, Nucl. Phys. B350 (1991) 201.
15. M. Campostrini, A. Di Giacomo, H. Panagopoulos, Phys. Lett. B212 (1988) 206.
16. B. Allés, E. Vicari, Phys. Lett. B268 (1991) 241.
17. M. Campostrini, A. Di Giacomo, H. Panagopoulos, E. Vicari, Nucl. Phys. B329 (1990) 683.
18. A. Di Giacomo, E. Vicari, Phys. Lett. B275 (1992) 419.
19. B. Allés, M. Campostrini, A. Di Giacomo, Y. Gündüç, E. Vicari, Phys. Rev. D48 (1993) 2284.
20. R. D. Pisarski, F. Wilczek, Phys. Rev. D29 (1984) 338.
21. J. I. Skullerud, S. Hands, S. Kim, hep-lat/0511001; D. Toublan, A. R. Zhitnitsky, hep-ph/0503256.
22. H. Kluberg-Stern, A. Morel, O. Napoly, B. Petersson, Nucl. Phys. B220 (1983) 447.